JACS
JOURNAL OF THE AMERICAN CHEMICAL SOCIETY
Communication
pubs.acs.org/JACS

Rapid Macrocycle Threading by a Fluorescent Dye–Polymer Conjugate in Water with Nanomolar Affinity

Evan M. Peck,[†] Wenqi Liu,[†] Graeme T. Spence,[†] Scott K. Shaw,[†] Anthony P. Davis,*[,‡] Harry Destecroix,[‡] and Bradley D. Smith*[,†]

[†]Department of Chemistry and Biochemistry, University of Notre Dame, Notre Dame, Indiana 46556, United States
[‡]School of Chemistry, University of Bristol, Cantock's Close, Bristol BS8 1TS, U.K.

Supporting Information

ABSTRACT: A macrocyclic tetralactam host is threaded by a highly fluorescent squaraine dye that is flanked by two polyethylene glycol (PEG) chains with nanomolar dissociation constants in water. Furthermore, the rates of bimolecular association are very fast with $k_{on} \approx 10^6$–10^7 M^{-1} s^{-1}. The association is effective under cell culture conditions and produces large changes in dye optical properties including turn-on near-infrared fluorescence that can be imaged using cell microscopy. Association constants in water are ∼1000 times higher than those in organic solvents and strongly enthalpically favored at 27 °C. The threading rate is hardly affected by the length of the PEG chains that flank the squaraine dye. For example, macrocycle threading by a dye conjugate with two appended PEG2000 chains is only three times slower than threading by a conjugate with triethylene glycol chains that are 20 times shorter. The results are a promising advance toward synthetic mimics of streptavidin/biotin.

The binding pockets within biological receptors usually contain a mixture of hydrophobic and polar residues that act synergistically to drive shape-selective binding of target guest molecules.[1] A classic example is the remarkably strong binding of biotin by the streptavidin/avidin protein ($K_a \approx 10^{13-15}$ M^{-1}) which is achieved primarily by a mixture of hydrophobic interactions and a large number of hydrogen bonds.[2] One of the classic goals of supramolecular chemistry is to produce synthetic mimics of these remarkable binding systems; however, there are presently very few uncharged organic host–guest binding partners that associate in water with very high affinity. A 2003 literature survey by Houk and co-workers determined that the average K_a was $10^{3.4\pm1.6}$ M^{-1}.[3] Since then there have been several impressive demonstrations of high affinity binding of small molecule guests by cyclodextrin,[4] cucurbituril,[5] or cyclophane hosts.[6] These container molecules share a common barrel-like molecular architecture with a hydrophobic interior and a series of polar groups around the periphery of each portal. While these hosts have undoubted practical and scientific value, the spatial separation of hydrophobic and polar regions restricts the structural range of host–guest pairs that can be designed for selective recognition.[7] In 1991, Diederich articulated the molecular design concept of a rigid cyclophane host with a mixed cavity comprised of hydrophobic surfaces and inward directed hydrogen bonding residues.[8] He suggested that this type of biomimetic host architecture would bind complementary guests with high affinity and shape selectivity due to favorable enthalpic changes (Scheme 1).[9]

Scheme 1. Binding in Water by an Amphiphilic Cavity[a]

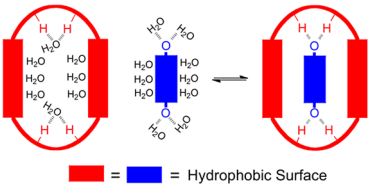

[a]Formation of host–guest hydrogen bonds compensates for the desolvation of polar groups and combines with desolvation of hydrophobic surfaces to produce strong complexation.[8]

Water-soluble hosts with amphiphilic cavities are relatively rare, with previous studies of calixpyrroles and oligolactam hosts in water reporting dissociation constants that are micromolar or above.[10] Here we describe a new water-soluble organic host–guest pair in which polar and hydrophobic interactions combine to give nanomolar dissociation constants. The supramolecular design is based on two previous discoveries. In 2007, we described the organic-soluble macrocyclic tetralactam host **M1** with two anthracene side walls (Scheme 2) and showed that it was able to encapsulate a deep-red fluorescent squaraine dye.[11] Each squaraine oxygen atom formed bifurcated hydrogen bonds with the proximal host amide NH residues, and there was complementary stacking of the host and guest aromatic surfaces. Binding constants were moderate at $\sim 10^6$ M^{-1}. In 2012, the water-soluble analogue **M2** was prepared and evaluated as a fluorescent host for monosaccharides.[12] The study also showed that the structure of empty **M2** is highly preorganized in aqueous solution; the four NH residues are forced by the adjacent peri hydrogens to point into the binding cavity. This observation prompted us to investigate if **M2** could bind water-soluble squaraine guests.

The squaraine dyes used in this study have chemical structures containing two electron-donating 2-aminothiophene units which diminish the electrophilicity of the central C_4O_2 core such that dyes **S1**–**S4** resist nucleophilic attack by the aqueous solvent.

Received: April 6, 2015
Published: June 24, 2015

DOI: 10.1021/jacs.5b03573
J. Am. Chem. Soc. 2015, 137, 8668–8671

Scheme 2. Compounds Studied

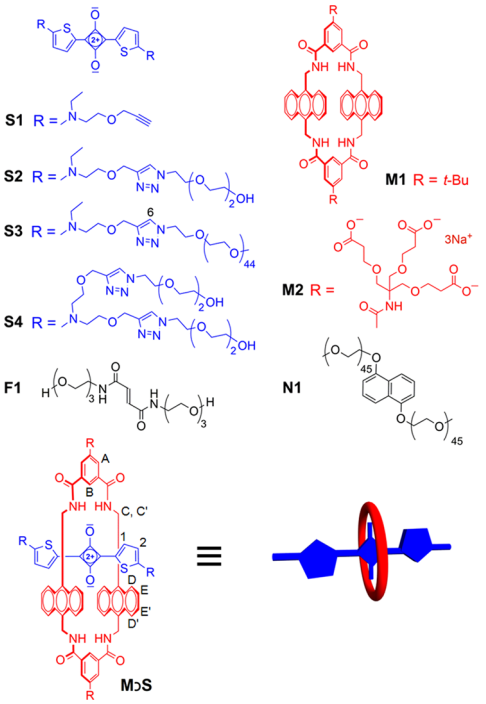

The improved chemical stability was a significant breakthrough that enabled accurate squaraine binding studies to be conducted in water. As expected for squaraine dyes, compounds **S1**−**S4** exhibit intense and narrow deep-red absorption and emission bands that make them very attractive for many types of optical imaging, sensing, and light harvesting applications.[13] Furthermore, the squaraine absorption and emission bands are red-shifted by 20−40 nm when the dye is encapsulated inside the tetralactam macrocycle, a diagnostic optical change that greatly facilitates association measurements.[11] The organic-soluble host **M1** and water-soluble **M2** have identical binding cavities and differ only in the peripheral appendages. The organic-soluble bisalkyne squaraine **S1** was prepared in a straightforward manner, and polyethylene glycol (PEG) chains of two different lengths were covalently attached to create structures **S2** and **S3** which were soluble in various organic solvents and water.

Host/guest complexation was studied in three solvents, chloroform, methanol, and water. In each case, macrocycle threading and dye encapsulation were indicated by diagnostic changes in NMR chemical shifts and absorption/fluorescence maxima bands, and fluorescence energy transfer from the macrocycle anthracene units to the encapsulated squaraine. In Figure 1 are partial ^{1}H NMR spectra showing the changes in chemical shift due to complexation of **S3** by **M2** to form **M2⊃S3** in D_2O. A ROESY spectrum confirmed the threaded structure with a through-space correlation between the macrocycle anthracene protons E and E′ and the thiophene protons 1 and 2. Analogous NMR experiments to form **M1⊃S1** in $CDCl_3$ and **M2⊃S1** in CD_3OD are described in the Supporting Information. In each case, the changes in chemical shift are consistent with the aromatic stacking and hydrogen bonding effects caused by dye encapsulation inside the macrocycle. For example, the squaraine thiophene protons 1 and 2 move upfield whereas the macrocycle proton B moves downfield. The squaraine dyes exist as conformational isomers, based on the relative orientation of the thiophene units (*cis* or *trans*), and the NMR studies revealed

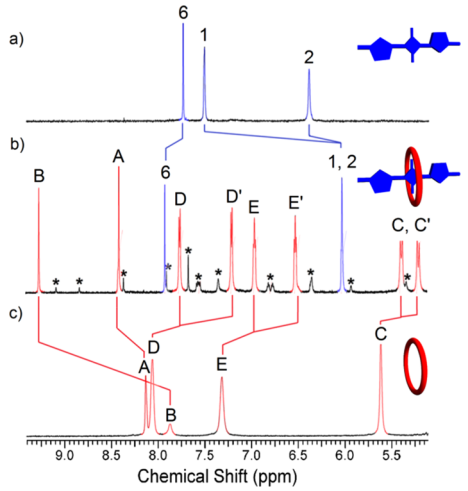

Figure 1. Partial ^{1}H NMR (600 MHz, D_2O, 25 °C) of (a) squaraine dye **S3** (2.0 mM); (b) complex **M2⊃S3** (2.0 mM); and (c) empty macrocycle **M2** (2.0 mM). * designates NMR signals for the minor **M2⊃S3** complex with encapsulated **S3** in a *cis* conformation (*trans*/*cis* ratio for encapsulated **S3** ∼10:1).

that the *trans* squaraine isomer was the major isomer encapsulated by the macrocycle (see Supporting Information for a computational model of the host/guest complex and further discussion of the squaraine *cis*−*trans* isomerization).

The red-shifted squaraine absorption and emission bands made it straightforward to monitor macrocycle threading and dye encapsulation (Figure 2). For example, encapsulation of **S3** by **M2** moved the squaraine absorbance maxima to 678 nm and the sample solution exhibited a distinct color change from blue to green. There was also an increase in fluorescence quantum yield, and both factors combined to produce a very large switch-on fluorescence effect at the red-shifted emission wavelength of 712 nm (Figure 2d). Additional evidence for squaraine complexation

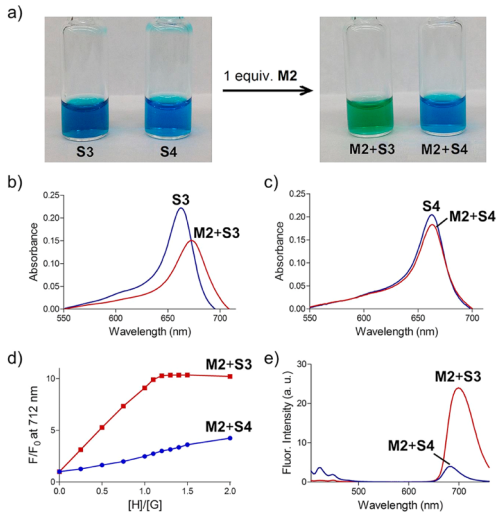

Figure 2. Comparison of the optical changes in H_2O. (a) Color change achieved by adding **M2** to separate equimolar solutions of **S3** or control dye **S4** (200 μM each); (b) absorbance spectrum of **S3** (3.0 μM) or **M2** + **S3** (3.0 μM each); (c) absorbance spectrum of **S4** (3.0 μM) or **M2** + **S4** (3.0 μM each); (d) fluorescence titration (ex: 690 nm, em: 712) of **M2** into separate solutions of **S3** or **S4** (1.0 μM); (e) fluorescence emission upon excitation of **M2** anthracene band (ex: 390 nm) in separate samples of **M2** + **S3** or **M2** + **S4** (1.0 μM each).

DOI: 10.1021/jacs.5b03573
J. Am. Chem. Soc. 2015, 137, 8668−8671

was the observation of efficient energy transfer from an excited anthracene unit in **M2** (ex: 390 nm) to the encapsulated squaraine dye (em: 712 nm) (Figure 2e).[11] In contrast, these substantial optical changes did not occur when **M2** was mixed with the control dye **S4** because macrocycle threading was blocked by the pair of split triethylene glycol chains that flanked the dye structure.[14] A final piece of evidence for complete encapsulation of **S3** by **M2** was increased resistance to chemical bleaching of the squaraine color by a highly nucleophilic sulfide dianion.[15] In agreement with previous observations, addition of excess Na_2S to free squaraine dye **S3** produced a 55% decrease in squaraine absorbance over 20 min due to nucleophilic attack, whereas there was no decrease in squaraine color intensity when Na_2S was added to a sample of **S3** that had been premixed with **M2** (forming **M2⊃S3**) (Figure S11).

The complexation-induced changes in optical properties enabled titration experiments that measured kinetic and thermodynamic constants in three solvents, chloroform, methanol, and water. The weaker binding in chloroform and methanol was monitored by absorption, whereas the stronger binding in water was measured at lower concentration using fluorescence methods. As summarized in Table 1, host–guest

Table 1. Thermodynamic and Kinetic Data for Host/Guest Association at 20 °C

guest	host	solvent	K_a (M^{-1})	k_{on} (M^{-1} s^{-1})
S1	**M1**	$CHCl_3$	$(5.9 \pm 1.6) \times 10^5$	8.6 ± 0.4
S3	**M1**	$CHCl_3$	$(2.0 \pm 0.5) \times 10^6$	11.9 ± 0.9
S1	**M2**	MeOH	$(4.0 \pm 0.6) \times 10^5$	$(1.2 \pm 0.1) \times 10^4$
S2	**M2**	MeOH	$(4.0 \pm 0.6) \times 10^5$	$(1.8 \pm 0.2) \times 10^3$
S3	**M2**	MeOH	$(4.1 \pm 1.0) \times 10^5$	$(5.1 \pm 0.6) \times 10^3$
S2	**M2**	H_2O	$(6.0 \pm 1.2) \times 10^8$	$(1.2 \pm 0.1) \times 10^7$
S3	**M2**	H_2O	$(1.1 \pm 0.4) \times 10^9$	$(4.3 \pm 0.3) \times 10^6$
F1	**M2**	H_2O	$(1.6 \pm 0.1) \times 10^4$	–

binding in the organic solvents was moderate ($K_a = (0.4–2.0) \times 10^6$ M^{-1}) and comparable to previous reports using analogous squaraine dyes.[11] However, the association constants in water were ~1000 times higher. For example, the association constant to form **M2⊃S3** in water was 1.1×10^9 M^{-1} at 20 °C. This remarkably strong association was confirmed by independent guest displacement experiments. Guided by literature precedent,[16] we prepared the water-soluble bis-fumaride **F1** and determined by NMR and fluorescence titration experiments with **M2** that a 1:1 complex was formed with $K_a = 1.6 \times 10^4$ M^{-1} at 20 °C (Figures S19 and S20). Competitive titration experiments were then conducted that added **S3** to a sample of **M2⊃F1** and observed unambiguous fluorescence and NMR evidence for displacement of **F1** from the macrocycle and confirmation of nanomolar affinity for **M2⊃S3** (Figures S21 and S23).

To gain additional thermodynamic insight, the aqueous titrations were repeated and monitored by Isothermal Titration Calorimetry (ITC) at 27 °C (Figures S24–S27). Association of **M2** and **F1** was determined to be highly favored enthalpically ($\Delta H = -11.3$ kcal/mol) and moderately disfavored entropically ($T\Delta S = -5.1$ kcal/mol). The association constant for **M2** and **S3** was too high for accurate measurement using our microcalorimeter, but a single injection experiment determined ΔH to be −11.7 kcal/mol. A fluorescence titration experiment at this temperature provided $\Delta G = -11.3$ kcal/mol and thus $T\Delta S = -0.4$ kcal/mol. These thermodynamic data support a model where **F1** and **S3** both form enthalpically favored hydrogen bonds with the four NH residues inside **M2**, a picture that is supported by computational modeling (Figure S4) and several analogous X-ray crystal structures.[11,16–18] The structure of squaraine **S3** is more rigid and more hydrophobic than fumaride **F1** which is likely a major reason why complexation of **S3** does not suffer as large an entropic penalty.

The initial rates of host–guest association, k_{on}, were measured using standard fluorescence or absorption methods (see Supporting Information). Association in chloroform was slow enough for standard mixing experiments in a single cuvette, but the much faster formation of **M2⊃S3** in methanol and water required stopped-flow instrumentation. Inspection of the rate constants in Table 1 reveals two notable trends. One is that the initial rate constant for association of **M2** with squaraine dye **S3** in water ($k_{on} = (4.3 \pm 0.3) \times 10^6$ M^{-1} s^{-1} which corresponds to a half-life of 7 s when both components are mixed at 30 nM) is almost 1000 times faster than the same process in methanol and >300 000-fold faster than the rate constant for analogous association of **M1** with **S3** in chloroform (Table 1). The lubricating effect of water was further investigated by measuring the rates of association in water/methanol mixtures.[19] The rate of association increased dramatically once the mole fraction of water was >0.9 (Figure S34). Another notable trend in Table 1 is that the length of the ethylene glycol chains at the ends of the squaraine dye does not greatly affect the rate of macrocycle threading in any specific solvent. For example, threading of **M2** by **S2** in water, which requires macrocycle passage along a relatively short triethylene glycol chain, is only three times faster than threading by **S3**, which requires macrocycle passage along a PEG2000 chain that is 20 times longer.

The threading of cyclodextrin and cucurbituril by long PEG chains in water is well-known,[20] and threading of cucurbituril by a dye flanked with PEG chains has also been reported.[21] In addition, an organic-soluble threaded macrocycle/polymer system has been studied in detail.[22] In comparison, the high affinities and rapid kinetics of the current association system are noteworthy, and so are the large ratiometric changes in near-infrared optical properties, including turn-on fluorescence. The potential utility of these properties was demonstrated by conducting fluorescence imaging studies of Chinese Hamster Ovary (CHO) cells that had been incubated for 8 h at 37 °C in culture media with **S3** or a mixture of **M2** + **S3**.[23] The live cell micrographs in Figure 3 show that uptake of **S3** into intracellular endosomes is visualized using a Red excitation/emission filter set, whereas endosomal uptake of **M2⊃S3** is observed selectively

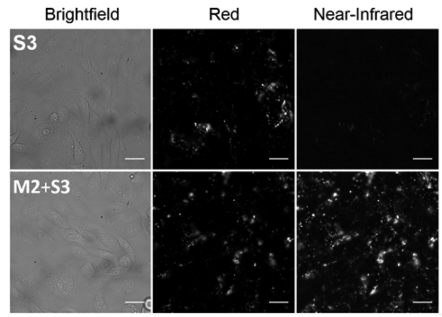

Figure 3. Micrographs of live CHO cells in culture media at 8 h after treatment with (top row) **S3** (10 μM); (bottom row) mixture of **M2** + **S3** (10 μM each). Epifluorescence images acquired using Red (ex: 620 ± 60 nm, em: 700 ± 75 nm) or Near-Infrared (ex: 710 ± 75 nm, em: 810 ± 90 nm) filter sets. Scale bar = 10 μm.

DOI: 10.1021/jacs.5b03573
J. Am. Chem. Soc. 2015, 137, 8668–8671

using a Near-Infrared filter set. The **M2⊃S3** complex can also be imaged microscopically or on the mesoscale using an alternative filter set that excites the surrounding anthracene units with blue light and detects near-infrared emission from the encapsulated squaraine dye (Figures S36−S37). A time-resolved movie of the live cells containing **M2⊃S3** clearly shows the expected endosome tracking (see Supporting Information). These imaging results demonstrate that the **M2⊃S3** complex is stable in complex biological environments and can be selectively visualized by different types of fluorescence imaging protocols.

In conclusion, we report a host−guest pair which employs an amphiphilic cavity to achieve nanomolar binding in water. The structures of both components are readily tunable, and conjugation to biomolecules or surfaces should also be straightforward, leading to optically active alternatives to the streptavidin−biotin association system. The distinctive recognition properties of the host−guest pair suggest orthogonality to other strong binding pairs (e.g., cucurbituril/alkylammonium),[5] and hence the potential for simultaneous use. The ability to engineer multiple strong but controllable noncovalent interactions raises interesting possibilities for applications in biomedical science, materials science, and nanotechnology.

■ ASSOCIATED CONTENT

Supporting Information

Chemical synthesis and characterization, thermodynamic and kinetics data, cell imaging. The Supporting Information is available free of charge on the ACS Publications website at DOI: 10.1021/jacs.5b03573.

■ AUTHOR INFORMATION

Corresponding Authors

*smith.115@nd.edu

*anthony.davis@bristol.ac.uk

Notes

The authors declare no competing financial interest.

■ ACKNOWLEDGMENTS

Financial support for this work was provided by the University of Bristol's EPSRC Impact Acceleration Account, the NSF (CHE1401783), the NIH (T32GM075762), and a Walther Cancer Foundation Advancing Basic Cancer Research Grant administered by the Harper Cancer Research Institute (USA).

■ REFERENCES

(1) (a) Persch, E.; Dumele, O.; Diederich, F. *Angew. Chem., Int. Ed.* **2015**, *11*, 3290. (b) Zhao, Y. *ChemPhysChem* **2013**, *14*, 3878. (c) Homans, S. W. *Drug Discovery Today* **2007**, *12*, 534. (d) Lemieux, R. U. *Acc. Chem. Res.* **1996**, *29*, 373.

(2) (a) Stayton, P. S.; Freitag, S.; Klumb, L. A.; Chilkoti, A.; Chu, V.; Penzotti, J. E.; To, R.; Hyre, D.; Le Trong, I.; Lybrand, T. P. *Biomol. Eng.* **1999**, *16*, 39. (b) Klumb, L. A.; Chu, V.; Stayton, P. S. *Biochemistry* **1998**, *37*, 7657. (c) Weber, P. C.; Ohlendorf, D.; Wendoloski, J.; Salemme, F. *Science* **1989**, *243*, 85.

(3) Houk, K.; Leach, A. G.; Kim, S. P.; Zhang, X. *Angew. Chem., Int. Ed.* **2003**, *42*, 4872.

(4) (a) Grishina, A.; Stanchev, S.; Kumprecht, L.; Budějínský, M.; Pojarová, M.; Dušek, M.; Rumlová, M.; Křížová, I.; Rulíšek, L.; Kraus, T. *Chem.—Eur. J.* **2012**, *18*, 12292. (b) Uhlenheuer, D. A.; Milroy, L.-G.; Neirynck, P.; Brunsveld, L. *J. Mater. Chem.* **2011**, *21*, 18919. (c) Yang, Z.; Breslow, R. *Tetrahedron Lett.* **1997**, *38*, 6171.

(5) (a) Smith, L. C.; Leach, D. G.; Blaylock, B. E.; Ali, O. A.; Urbach, A. R. *J. Am. Chem. Soc.* **2015**, *137*, 3663. (b) Cao, L.; Šekutor, M.; Zavalij, P. Y.; Mlinarić-Majerski, K.; Glaser, R.; Isaacs, L. *Angew. Chem., Int. Ed.* **2014**, *53*, 988. (c) Masson, E.; Ling, X.; Joseph, R.; Kyeremeh-Mensah, L.; Lu, X. *RSC Adv.* **2012**, *2*, 1213. (d) Rekharsky, M. V.; Mori, T.; Yang, C.; Ko, Y. H.; Selvapalam, N.; Kim, H.; Sobransingh, D.; Kaifer, A. E.; Liu, S.; Isaacs, L. *Proc. Natl. Acad. Sci. U.S.A.* **2007**, *104*, 20737.

(6) (a) Hagiwara, K.; Akita, M.; Yoshizawa, M. *Chem. Sci.* **2015**, *6*, 259. (b) Yu, G.; Zhou, X.; Zhang, Z.; Han, C.; Mao, Z.; Gao, C.; Huang, F. *J. Am. Chem. Soc.* **2012**, *134*, 19489. (c) Venturi, M.; Dumas, S.; Balzani, V.; Cao, J.; Stoddart, J. F. *New J. Chem.* **2004**, *28*, 1032. (d) Gibb, C. L.; Gibb, B. C. *J. Am. Chem. Soc.* **2004**, *126*, 11408.

(7) Lehn, J. M. *Angew. Chem., Int. Ed.* **1988**, *27*, 89.

(8) Diederich, F. *Cyclophanes*; Royal Society of Chemistry: Cambridge, 1991; pp 261−263.

(9) Meyer, E. A.; Castellano, R. K.; Diederich, F. *Angew. Chem., Int. Ed.* **2003**, *42*, 1210.

(10) (a) Verdejo, B.; Gil-Ramírez, G.; Ballester, P. *J. Am. Chem. Soc.* **2009**, *131*, 3178. (b) Ferrand, Y.; Klein, E.; Barwell, N. P.; Crump, M. P.; Jiménez-Barbero, J.; Vicent, C.; Boons, G.-J.; Ingale, S.; Davis, A. P. *Angew. Chem., Int. Ed.* **2009**, *48*, 1775. (c) Ferrand, Y.; Crump, M. P.; Davis, A. P. *Science* **2007**, *318*, 619. (d) Hunter, C.; Thomas, J.; Bernad, P., Jr *Chem. Commun.* **1998**, *22*, 2449.

(11) (a) Gassensmith, J. J.; Arunkumar, E.; Barr, L.; Baumes, J. M.; DiVittorio, K. M.; Johnson, J. R.; Noll, B. C.; Smith, B. D. *J. Am. Chem. Soc.* **2007**, *129*, 15054.

(12) Ke, C.; Destecroix, H.; Crump, M. P.; Davis, A. P. *Nat. Chem.* **2012**, *4*, 718.

(13) (a) Avirah, R. R.; Jayaram, D. T.; Adarsh, N.; Ramaiah, D. *Org. Biomol. Chem.* **2012**, *10*, 911. (b) McEwen, J. J.; Wallace, K. J. *Chem. Commun.* **2009**, *45*, 6339. (c) Sreejith, S.; Carol, P.; Chithra, P.; Ajayaghosh, A. *J. Mater. Chem.* **2008**, *18*, 264.

(14) A simple TLC study showed that the presence of **M2** completely prevented elution of **S3**, indicating formation of a very polar **M2⊃S3** complex, but the presence of **M2** had no effect on the retention factor of **S4**, indicating that a threaded complex was not formed (see Figure S12).

(15) Arunkumar, E.; Forbes, C. C.; Noll, B. C.; Smith, B. D. *J. Am. Chem. Soc.* **2005**, *127*, 3288.

(16) Gatti, F. G.; Leigh, D. A.; Nepogodiev, S. A.; Slawin, A. M. Z.; Teat, S. J.; Wong, J. K. Y. *J. Am. Chem. Soc.* **2001**, *123*, 5983.

(17) Gassensmith, J. J.; Baumes, J. M.; Smith, B. D. *Chem. Commun.* **2009**, *45*, 6329.

(18) We also characterized the association of control guest **N1** with **M2** in water. The naphthalene core of **N1** has two attached oxygen atoms with similar spacing as the two oxygens in **S3** and **F1**, but with much weaker hydrogen bond accepting ability. ^{1}H NMR chemical shift data indicated threading of **N1** by **M2** (Figure S8), and ITC titration studies in water at 27 °C determined that a 1:1 complex was formed with K_a = 7.7 ×10^3 M^{-1}, ΔH = −5.9 kcal/mol, and $T\Delta S$ = 0.8 kcal/mol (Figure S27). The change in guest from **S3** (or **F1**) to **N1** thus lowers the enthalpic driving force by ∼6 kcal/mol. It seems likely that part of this is due to the weaker hydrogen bonding of **N1** with the four NH residues inside **M2**, although other factors presumably contribute since the structures of **S3**, **F1**, and **N1** have different hydrophobic surface areas and hydration shells. For a recent discussion of these factors, see: Biedermann, F.; Nau, W. M.; Schneider, H. J. *Angew. Chem., Int. Ed.* **2014**, *53*, 11158.

(19) Panman, M. R.; Bakker, B. H.; den Uyl, D.; Kay, E. R.; Leigh, D. A.; Buma, W. J.; Brouwer, A. M.; Geenevasen, J. A.; Woutersen, S. *Nat. Chem.* **2013**, *5*, 929.

(20) (a) Harada, A.; Takashima, Y.; Yamaguchi, H. *Chem. Soc. Rev.* **2009**, *38*, 875. (b) Buschmann, H.-J.; Jansen, K.; Schollmeyer, E. *J. Incl. Phenom. Macrocycl. Chem.* **2000**, *37*, 231.

(21) (a) Biedermann, F.; Elmalem, E.; Ghosh, I.; Nau, W. M.; Scherman, O. A. *Angew. Chem., Int. Ed.* **2012**, *51*, 7739.

(22) (a) Deutman, A. B. C.; Cantekin, S.; Elemans, J. A. A. W.; Rowan, A. E.; Nolte, R. J. M. *J. Am. Chem. Soc.* **2014**, *136*, 9165. (b) Deutman, A. B. C.; Monnereau, C.; Elemans, J. A. A. W.; Ercolani, G.; Nolte, R. J. M.; Rowan, A. E. *Science* **2008**, *322*, 1668.

(23) Cell vitality assays showed no evidence of toxicity for concentrations of **S1**, **S3**, and **M2** up to 50 μM (see Figure S35).

DOI: 10.1021/jacs.5b03573
J. Am. Chem. Soc. 2015, 137, 8668−8671